Nuclear Engineering and Technology 53 (2021) 1429–1435

Contents lists available at ScienceDirect

Nuclear Engineering and Technology

journal homepage: www.elsevier.com/locate/net

Original Article

Numerical analysis of the temperature distribution of the EM pump for the sodium thermo-hydraulic test loop of the GenIV PGSFR

Jaesik Kwak, Hee Reyoung Kim*

Ulsan National Institute of Science and Technology, 50, UNIST-gil, Ulsan, 44919, Republic of Korea

ARTICLE INFO

Article history:
Received 3 February 2020
Received in revised form
12 November 2020
Accepted 15 November 2020
Available online 26 November 2020

Keywords:
Electromagnetic pump
Temperature distribution
Heat transfer
Numerical analysis
PGSFR
IHTS

ABSTRACT

The temperature distribution of an electromagnetic pump was analyzed with a flow rate of 1380 L/min and a pressure of 4 bar designed for the sodium thermo-hydraulic test in the Sodium Test Loop for Safety Simulation and Assessment-Phase 1 (STELLA-1). The electromagnetic pump was used for the circulation of the liquid sodium coolant in the Intermediate Heat Transport System (IHTS) of the Prototype Gen-IV Sodium-cooled Fast Reactor (PGSFR) with an electric power of 150 MWe. The temperature distribution of the components of the electromagnetic pump was numerically analyzed to prevent functional degradation in the high temperature environment during pump operation. The heat transfer was numerically calculated using ANSYS Fluent for prediction of the temperature distribution in the excited coils, the electromagnet core, and the liquid sodium flow channel of the electromagnetic pump. The temperature distribution of operating electromagnetic pump was compared with cooling of natural and forced air circulation.

The temperature in the coil, the core and the flow gap in the two conditions, natural circulation and forced circulation, were compared. The electromagnetic pump with cooling of forced circulation had better efficiency than natural circulation even considering consumption of the input power for the air blower. Accordingly, this study judged that forced cooling is good for both maintenance and efficiency of the electromagnetic pump.

1. Introduction

An electromagnetic pump has been developed from 20th century for the purpose of transporting electrically conducting fluids, such as liquid metal. The electromagnetic pump transports liquid metal using the Lorenz force, which is calculated by the vector product of the current and the magnetic field, so it does not need an impeller [1–3]. The pump without an impeller has a simpler structure, a smaller size, and lower maintenance against the corrosiveness of liquid metals such as lead or sodium [4]. Due to those advantages of electromagnetic pump, it was chosen to be used for transporting the sodium coolant in the Intermediate Heat Transport System (IHTS) of a Prototype Generation-IV Sodium-cooled Fast Reactor (PGSFR) that is being developed in Korea [5–7].

However, in terms of the operation of electromagnetic pump in the nuclear reactor system, the input power required in the electromagnetic pump for the transportation of liquid sodium with a large flow rate against a high pressure loss [8,9] became too high and therefore it generated a large amount of heat due to Ohmic loss in the cores and coils. In order to reduce heat production due to eddy current generation, an insulating laminated core is generally used. Because the Curie temperature of the core is as high as 1073 K and the liquid metal temperature of operation is near 573 K, there is no magnetic deterioration in the rated operating temperature in the core. The electrical resistivity and mechanical strength of driving coils, which are positioned close to the high temperature sodium environment, is an important factor for performance of an electromagnetic pump, so the temperature of coils must be maintained at below the appropriate point [10].

The Intermediate Heat Exchanger (IHX) of the PGSFR is a counter-current flow type heat exchanger which transports heat from the sodium coolant of the Primary Heat Transport System (PHTS) to the Intermediate Heat Transport System (IHTS) [11,12]. Because the IHX has a dominant impact on the performance of the heat transport system of the PGSFR, performance of the components of the sodium thermo-hydraulic test system must be verified in the environment of the sodium flow. The heat exchange on the

* Corresponding author.
E-mail address: kimhr@unist.ac.kr (H.R. Kim).

https://doi.org/10.1016/j.net.2020.11.015

Nomenclature

A	Area [m^2]
B	Magnetic flux density [T]
C	Thermal capacity [$kg \cdot m^2/K \cdot s^2$]
E	Electric field [V/m]
H	Magnetic field strength [A/m]
h	Thermal convection coefficient [W/$m^2 \cdot K$]
J	Current density [A/m^2]
k	Thermal conductivity [W/$m \cdot K$]
n	Axial position in the boundary condition model of electromagnetic pump
Q	Heat quantity [J/s]
q	Heat quantity per time [J/s]
T	Temperature [K]
$\overrightarrow{u}$	Velocity [m/s]
ρ	Density [kg/m^3]
μ	Magnetic permeability [H/m]
ω	Input angular frequency [Hz]

components of the coolant system and the heat transfer in the IHX must be identified by an appropriate simulation in the sodium flow environment. An electromagnetic pump with a flow rate of 1380 L/min and pressure of 4 bar was designed for the sodium thermo-hydraulic experiment at the Sodium Test Loop for Safety Simulation and Assessment-Phase 1 (STELLA-1) which was constructed in the Korea Atomic Energy Research Institute (KAERI) as shown in Fig. 1 and Fig. 2.

We used the generation of heat in the components of the electromagnetic pump during operation from the results of a previous study [3] which examined the electromagnetic characteristics and performance of the same electromagnetic pump.

In this study, we solved the conduction and convection equations by solid components and air, respectively, using ANSYS Fluent, which is a commercially used numerical analysis code. We analyzed the temperature distribution of the designed electromagnetic pump considering heat generation and transfer in several cooling conditions. The results indicated the appropriate cooling conditions from the change of temperature distribution.

2. Theoretical approach

The design and principle of the electromagnetic force generated in an MHD pump are shown in Fig. 3 and Fig. 4. It consists of (1) at least one inductor where coils are embedded in a laminated ferromagnetic core, (2) an annular channel where liquid metal flows in the direction of the traveling magnetic field and (3) an inner ferromagnetic core or secondary inductor. The purpose of this construction was to generate a perpendicular (radial) component of traveling magnetic field by applying a three phase current to the coils. This form of the magnetic field induced currents in a liquid metal and the cross-product created generated the electromagnetic force in the direction of the traveling field.

For the generation of the axial traveling transverse magnetic field, we set the circumferential current density as in Eq. (1) based on the boundary conditions model of the electromagnetic pump in Fig. 5.

$$J_\theta(z) = \begin{cases} J_\theta Re\left[e^{iwtazAA}\right] \left(z_{6n+1,t} \le z \le z_{6n+1,b}\right) \\ -J_\theta Re\left[e^{iwt-\frac{4}{3}\pi}\right] \left(z_{6n+2,t} \le z \le z_{6n+2,b}\right) \\ J_\theta Re\left[e^{iwt-\frac{2}{3}\pi}\right] \left(z_{6n+3,t} \le z \le z_{6n+3,b}\right) \\ -J_\theta Re\left[e^{iwt}\right] \left(z_{6n+4,t} \le z \le z_{6n+4,b}\right) \\ J_\theta Re\left[e^{iwt-\frac{4}{3}\pi}\right] \left(z_{6n+5,t} \le z \le z_{6n+5,b}\right) \\ -J_\theta Re\left[e^{iwt-\frac{2}{3}\pi}\right] \left(z_{6n+6,t} \le z \le z_{6n+6,b}\right) \end{cases} \quad wheren = 0,1,2,3,4 \tag{1}$$

The circumferential current density in the real coil arrangement (J) induced magnetic field (B) and electric field intensity (E) which have the function of sinusoidal form temporally as seen in Eq. (2) in the other components of electromagnetic pump [13–15].

$$\begin{aligned} J(r,\theta,z) &= Re\left[J_\theta e^{iwt}\right]\widehat{\theta} \\ \mathrm{B}(r,\theta,z) &= Re\left[(B_r\widehat{r} + B_\theta\widehat{\theta} + B_z\widehat{z})e^{iwt}\right] \\ \mathrm{E}(r,\theta,z) &= Re\left[(E_r\widehat{r} + E_\theta\widehat{\theta} + E_z\widehat{z})e^{iwt}\right] \end{aligned} \tag{2}$$

The results of the induced magnetic field were derived as in Eq. (3) and Eq. (4) by solving Maxwell's equation in the cylindrical coordinates, and the results of the induced electric field intensity were derived as Eq. (5) by similar methods. The generation of heat by Ohmic loss in the components of the electromagnetic pump was calculated based on circumferential current density in Eq. (1) and

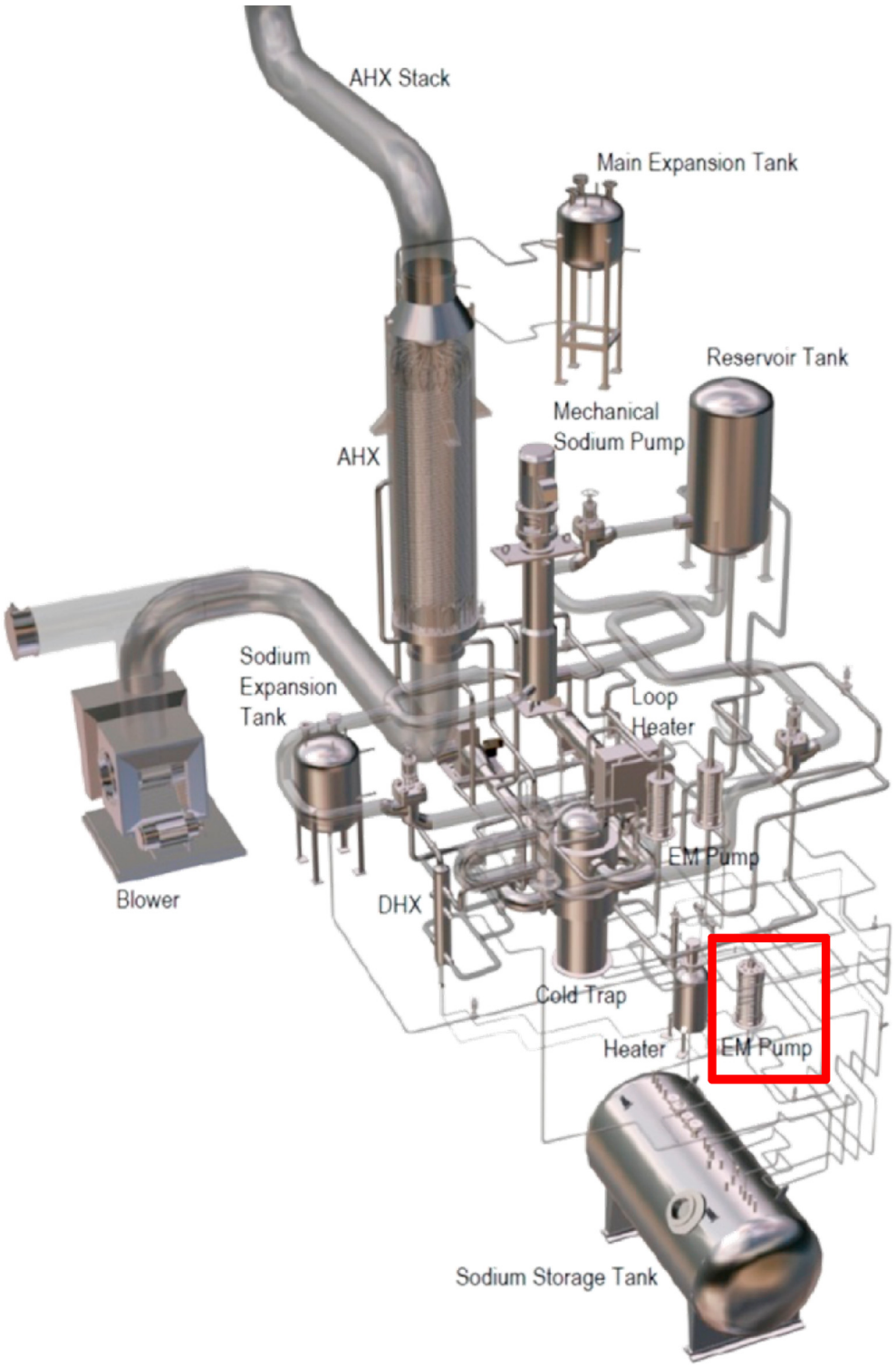

Fig. 1. Conceptual design of STELLA-1.

electric field intensity in Eq. (5).

$$\frac{\partial}{\partial r}\frac{1}{r}\left(B_r + r\frac{\partial B_r}{\partial r}\right) + \frac{\partial^2 B_r}{\partial z^2} = \mu\frac{\partial J_\theta}{\partial z} \tag{3}$$

$$\frac{1}{r}\frac{\partial B_z}{\partial r} + \frac{\partial^2 B_z}{\partial r^2} + \frac{\partial^2 B_z}{\partial z^2} = -\mu\left(\frac{1}{r}J_\theta + \frac{\partial J_\theta}{\partial r}\right) \tag{4}$$

$$\frac{\partial E_\theta}{\partial z} = iwB_r, \quad \frac{\partial E_r}{\partial z} - \frac{\partial E_z}{\partial r} = -iwB_\theta, \quad \frac{1}{r}\left(E_z + r\frac{\partial E_z}{\partial r}\right) = -iwB_z \tag{5}$$

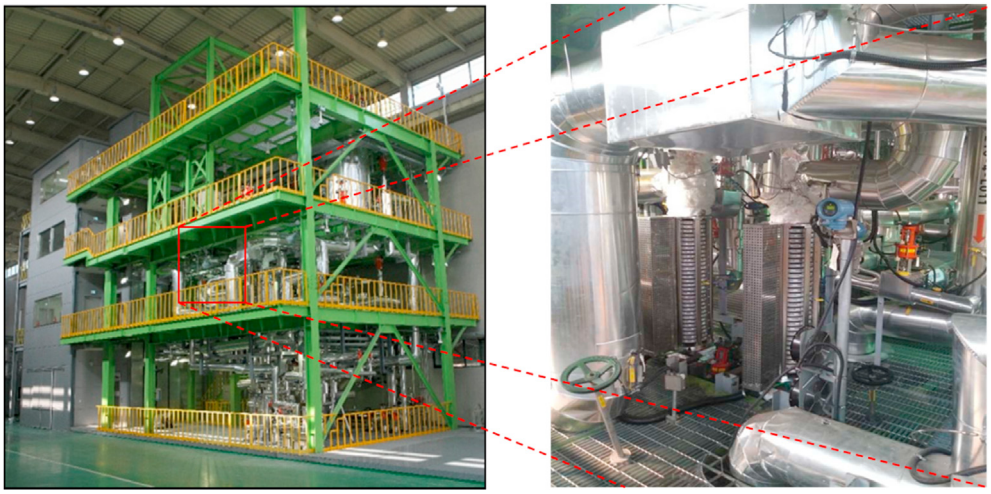

Fig. 2. Overall view of STELLA-1.

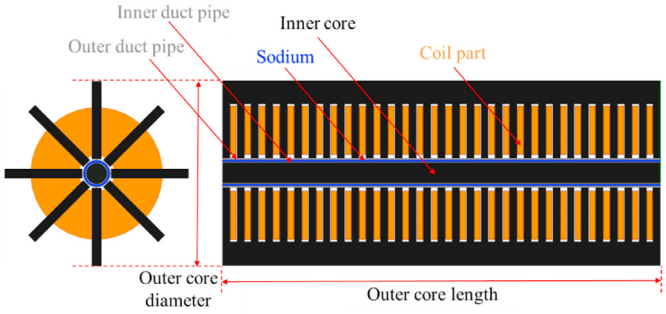

Fig. 3. Cross section of the electromagnetic pump.

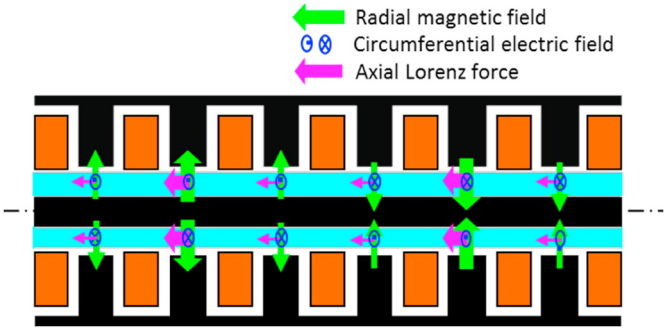

Fig. 4. Operation of the MHD pump.

Heat transfer with the conditions of the structural analysis using Eqs. (6) and (7) with a constant convection coefficient is simple, but that cannot express movement of a fluid, such as the cooling of natural circulation. As an advanced method, both the energy transportation equation and the movement of fluid based on the finite volume method was considered as Eq. (8). That calculated the temperature and velocity of the fluid near the solid, and the convection coefficient and outside temperature are defined and the amount of heat transfer was applied.

$$\vec{q} = -k\nabla T \tag{6}$$

$$\frac{dQ}{dt} = h \cdot A(T_o - T(t)) \tag{7}$$

$$\rho C\left(\frac{\partial T}{\partial t} + (\vec{u} \cdot \nabla)T\right) - \nabla \cdot (k - \nabla T) = \rho q \tag{8}$$

The type of convection is classified as natural convection in which fluid moves due to buoyancy effects, boiling convection in which the body is hot enough to cause a fluid phase change, and forced convection in which flow is induced by some external means. Different from other convection types, natural convection must be calculated delicately based on the Boussinesq model. The Boussinesq model must be used on the body force weighted condition.

The generation of heat from Ohmic loss were applied to each component and the heat transfer equation was applied to the 3 m × 3 m × 3 m space encasing the electromagnetic pump. The temperature of sodium in the flow gap was set as a constant of 613 K considering the flow conditions of sodium. Fig. 6 shows a 3D model of the electromagnetic pump for the numerical analysis.

3. Results and discussion

The quantity of generated heat by Ohmic loss in the electromagnetic pump components was calculated using ANSYS Maxwell; the heat distribution is presented in Fig. 7 and quantity of generated heat is presented in Table 1. A model of the 3 m × 3 m × 3 m air space wrapping electromagnetic pump was transferred from ANSYS Maxwell to ANSYS Fluent as depicted in Fig. 8 and the specifications are presented in Table 2.

Fig. 9 shows the 3D temperature distribution of the operating electromagnetic pump in a steady state without cooling. The left side indicates the upper direction and the right side the bottom direction of the electromagnetic pump. Because of buoyancy effects, natural convection cooling occurs near the electromagnetic pump by the upper direction of air flow.

Fig. 10 compares the temperature distribution of the operating electromagnetic pump with natural circulation cooling in the axial direction in three positions, the centerline, flow gap, and 0.1 m distance from the center with a radius of the electromagnetic pump of about 0.2 m. Generally, the bottom of the electromagnetic pump is cooled well while the upper side is not cooled because of the hotter air there. There is little difference in temperature between

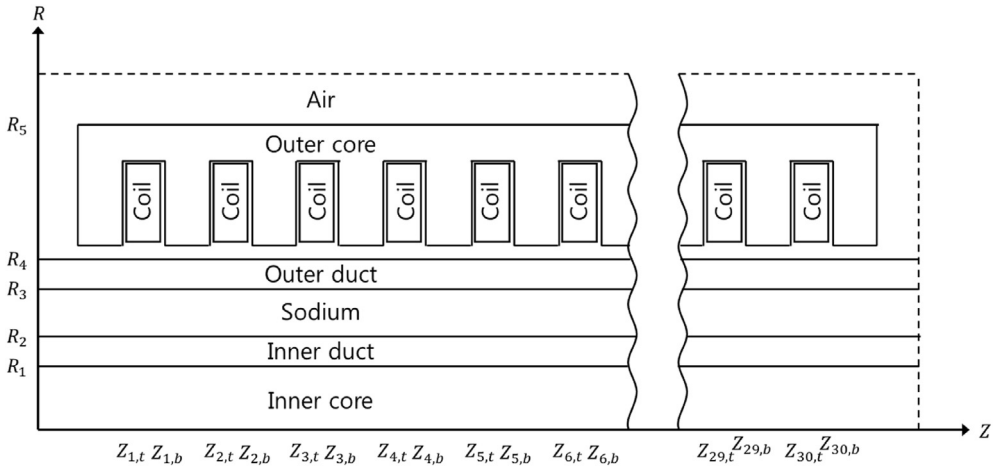

Fig. 5. Boundary conditions model of the electromagnetic pump.

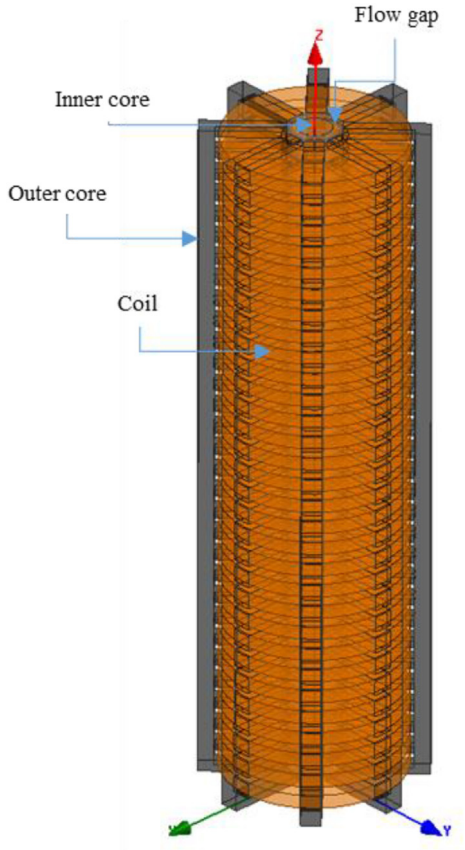

Fig. 6. 3D model of the electromagnetic pump.

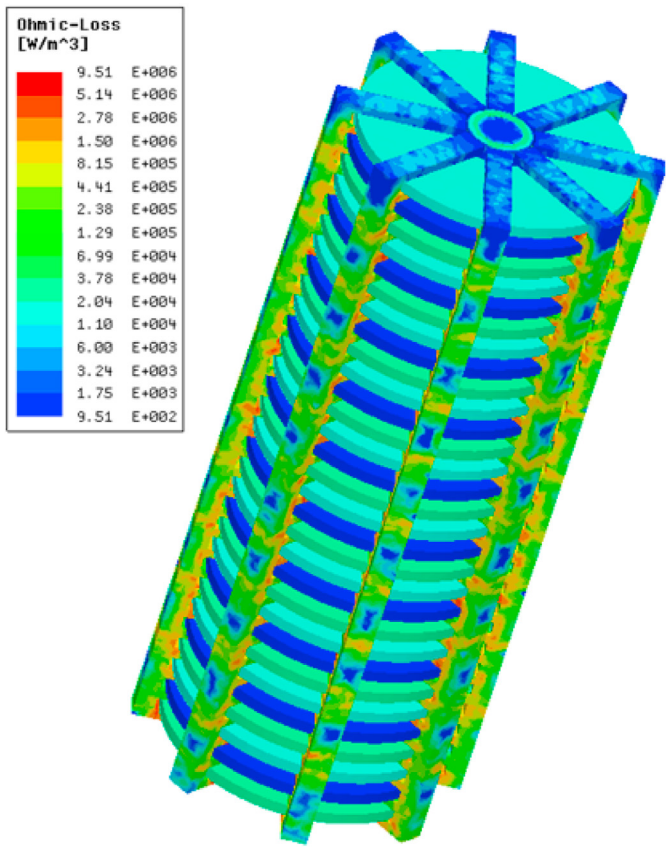

Fig. 7. Heat distribution in the electromagnetic pump.

the center and flow gap because conduction between the solid regions is less active. In the 0.1 m distance from the center, the temperature is decreased by about 100 K because the air gap between the duct and the coils disturbs the heat transfer in the radial direction.

Fig. 11 shows the temperature distribution of the operating electromagnetic pump in the steady state with forced cooling. To simulate forced convection cooling conditions in the 3 m × 3 m × 3 m space encasing the electromagnetic pump, there was a constant inlet of air with a velocity of 0.1 m/s in the four side directions,

Table 1
Generation of heat in the components of the electromagnetic pump.

	Volume [m^3]	Heat [W/m^3]
Inner core	0.00254	4.17 E+03
Inner duct	0.000302	4.44 E+05
Flow gap	0.00275	1.28 E+06
Outer duct	0.000567	3.24 E+05
One outer core	0.0029	2.71 E+05
One Coil	0.00236	1.18 E+04

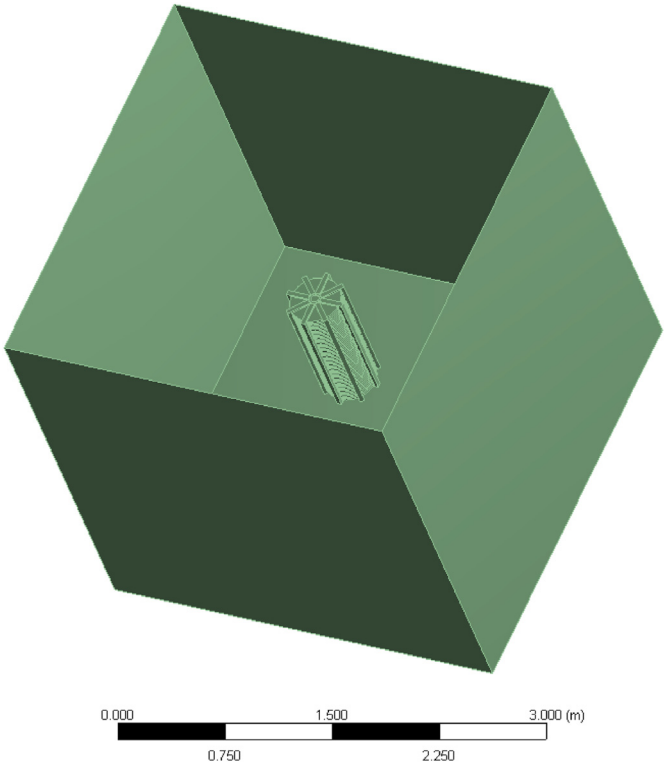

Fig. 8. 3 m × 3 m × 3 m space encasing electromagnetic pump.

while there were no special conditions in the upper and bottom directions. As a result, the temperature decreased because the cooling effect was stronger than the natural convection. The maximum temperature in the left bar was 613 K, which means that the components of the electromagnetic pump could not be hotter than the sodium in the flow gap.

In Fig. 12, the overall temperature distribution in the three positions of forced cooling is similar to that in Fig. 10, which shows the overall temperature distribution in the three positions of natural cooling. Although the temperature of the center and flow gap is similar to that of natural circulation as seen in Fig. 10, the maximum temperature of bottom is about 550 K, which is 60 K lower than in natural cooling conditions, and the upper side is about 610 K, which is 70 K lower than in natural cooling conditions.

After we analyzed the temperature distribution of the electromagnetic pump, we analyzed the performance of the electromagnetic pump again using ANSYS Maxwell based on the change in electrical resistivity of the components that is caused by a change in temperature. The results confirmed that the efficiency of the electromagnetic pump with forced circulation cooling was better than with natural circulation cooling by about 1.2%, which saves 1.31 kW of input power for operating the electromagnetic pump, which has a performance of a flow rate of about 1380 L/min and a developed pressure of 4.0 bar. Because electromagnetic parts of the electromagnetic pump are damaged by high temperature [16], forced cooling of the electromagnetic pump is necessary from the point of efficiency and maintenance.

4. Conclusion

In this study, we analyzed the temperature distribution of an electromagnetic pump with a flow rate of 1380 L/min and a developed pressure of 4 bar in both natural and forced cooling conditions. Forced cooling conditions show not only an overall decrease in temperature of about 70 K, but also an increase in efficiency of about 1.2% due to a change in the material properties of the electromagnetic pump components. A comparison of the

Table 2
Design specifications of the electromagnetic pump.

	Design variables	Unit	Values
Hydrodynamic	Flow rate	[L/min]	1380
	Mass flow	[kg/s]	20
	Developed pressure	[bar]	4.0
	Temperature	[K]	613
	Velocity	[m/s]	8.25
	Slip	[%]	42.7
	Reynolds number		360,158
	Head loss	[bar]	0.906
Geometrical	Core length	[mm]	1200
	Outer core diameter	[mm]	438
	inner core diameter	[mm]	57.2
	Inter core gap	[mm]	17.0
	Flow gap	[mm]	12.2
	Inner duct thickness	[mm]	1.65
	Outer duct thickness	[mm]	2.10
	Slot width	[mm]	27.7
	Slot depth	[mm]	117.7
	Core depth	[mm]	142.7
	Core thickness	[mm]	25.0
	Stacked coil thick	[mm]	101.2
	Coil support ring	[mm]	10.0
	Space in slot depth	[mm]	6.50
	Tooth width	[mm]	11.88
	Slot pitch	[mm]	39.6
	Conductor width	[mm]	23.72
	Conductor thickness	[mm]	2.00
	Insulator thickness	[mm]	0.20
Electrical	Input current	[A]	100
	Input voltage	[V]	1966
	Impedance	[Ohm]	19.7
	Input VA	[kVA]	340.6
	Input power	[kW]	109.4
	Power factor	[%]	32.1
	Goodness factor		2.3
	Pole pitch	[cm]	12.0
	Number of slot	[#]	30
	Turns/slot	[#]	46
	Number of pole pairs	[#]	5
	Slot/phase/pole	[#]	1

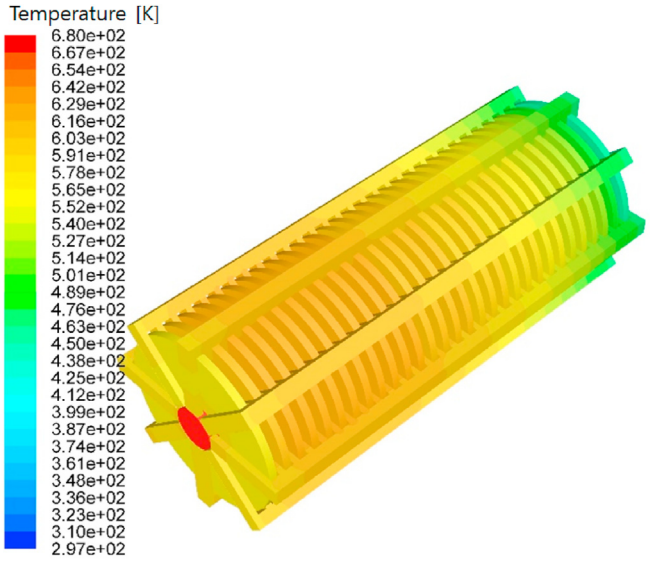

Fig. 9. 3D temperature distribution of the electromagnetic pump with natural circulation cooling.

Fig. 10. Temperature distribution of the electromagnetic pump with natural circulation cooling in the axial direction.

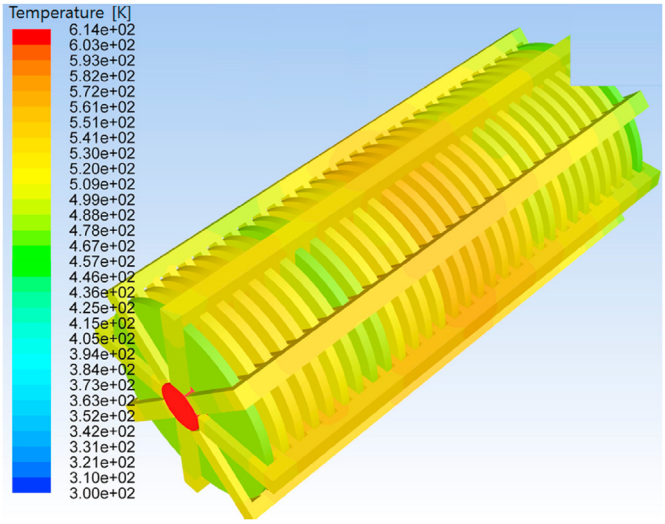

Fig. 11. 3D temperature distribution of the electromagnetic pump with forced circulation cooling.

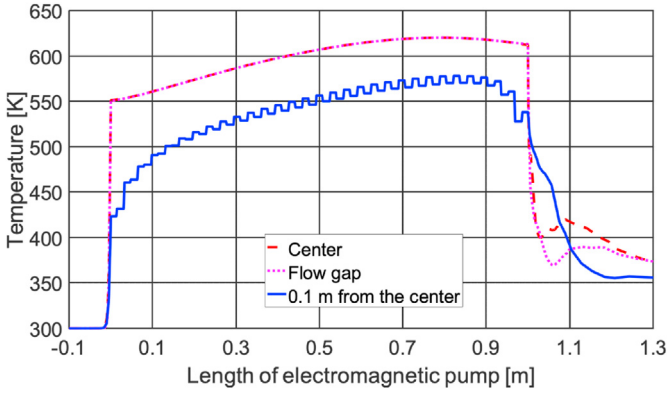

Fig. 12. Temperature distribution of the electromagnetic pump in the axial direction.

temperature distribution between the operation of the electromagnetic pump with cooling of forced air circulation and natural air circulation showed that the former was more suitable than the latter from the point of efficiency and maintenance.

Declaration of competing interest

The authors declare that they have no known competing financial interests or personal relationships that could have appeared to influence the work reported in this paper.

Acknowledgement

This work was supported by the National Research Foundation of Korea(NRF) grant funded by the Korea government(MSIT: Ministry of Science and ICT) (NRF-2019M2D1A1067205) and Korea Electric Power Corporation (Grant number: R18XA06-26).

References

[1] K. Aizawa, Y. Chikazawa, S. Kotake, K. Ara, R. Aizawa, H. Ota, Electromagnetic pumps for main cooling systems of commercialized sodium-cooled fast reactor, J. Nucl. Sci. Technol. 48 (3) (2011) 344–352.
[2] A.M. Andreev, et al., Results of an experimental investigation of electromagnetic pumps for the BOR-60 facility, Magnetohydrodynamics 4 (1978) 93–100.
[3] A.M. Andreev, et al., Choice of constructional schemes of electromagnetic pumps for atomic energy stations with fast reactors, Magnetohydrodynamics 1 (1982) 101–105.
[4] G.A. Baranov, et al., Calculation and Design of Liquid-Metal MHD Induction Machines, Atomizdat Publishers, Moscow, 1978.
[5] K. Bessho, S. Yamada, M. Nakano, K. Nakamoto, A new flux concentration type electromagnetic pump for FBR, J. Magn. Magn Mater. 112 (1) (1992) 419–422.
[6] S.K. Chang, et al., Flow distribution and pressure loss in sub channels of a wire-wrapped 37-pin rod bundle for a sodium-cooled fast reactor, Nuclear Engineering and Technology 48 (2) (2016) 376–385.
[7] P.A. Davidson, An Introduction to Magnetohydrodynamics, Cambridge University Press, Cambridge, 2001.
[8] D.H. Hahn, et al., Advanced SFR design concepts and R&D activities, Nuclear Engineering and Technology 41 (4) (2009) 427–446.
[9] Ota Hiroyuki, et al., Development of 160 m^3/min large capacity sodium-immersed self-cooled electromagnetic pump, J. Nucl. Sci. Technol. 41 (4) (2004) 511–523.
[10] International Atomic Energy Agency, Status of Innovative Fast Reactor Designs and Concepts. Advanced Reactor Information System, 2013.
[11] D.H. Kim, Y. Momozaki, C. Reed, Annular Linear Induction Pump (ALIP) Design Code Manual. ANL-KAERI-SFR-15-04, 2015.
[12] H.R. Kim, J.S. Kwak, MHD design analysis of an annular linear induction electromagnetic pump for SFR thermal hydraulic experimental Loop, Ann. Nucl. Energy 92 (2016) 127–135.
[13] H.R. Kim, Y.B. Lee, A design and characteristic experiment of the small annular linear induction electromagnetic pump, Ann. Nucl. Energy 38 (5) (2011) 1046–1052.
[14] S.A. Nasar, Linear Motion Electric Machines, John Wiley & Sons, New York, 1976.
[15] A. Oto, N. Naohara, M. Ishida, T. Kuroki, K. Katsuki, R. Kumazawa, Sodium-immersed self-cooled electromagnetic pump design and development of a large-scale coil for high temperature, Nuclear technology 110 (2) (1995) 159–167.
[16] C.C. Yang, S. Kraus, A large electro-magnetic pump for high temperature LMFBR applications, Nucl. Eng. Des. 44 (3) (1977) 383–395.